International Journal of Heat and Mass Transfer 52 (2009) 1510–1516

Contents lists available at ScienceDirect

International Journal of Heat and Mass Transfer

journal homepage: www.elsevier.com/locate/ijhmt

Numerical and experimental investigation of heat transfer on heating surface during subcooled boiling flow of liquid nitrogen

Xiangdong Li *, Wei Wei, Rongshun Wang, Yumei Shi

School of Mechanical Engineering, Shanghai Jiaotong University, 800 Dongchuan Road, Shanghai 200240, China

ARTICLE INFO

Article history:
Received 12 May 2007
Received in revised form 5 July 2008
Available online 1 October 2008

Keywords:
Liquid nitrogen
Subcooled boiling flow
The bubble departure diameter
The active site density
The bubble waiting time

ABSTRACT

Closure correlations describing bubble nucleation and departure on the heating surface is indispensable when modeling subcooled boiling flow using a two-fluid model. Due to the small contact angle and surface tension, nucleation and departure of nitrogen vapor bubble has different characteristics to those of high-boiling liquids. For the purpose of accurate two-fluid model formulation, these factors have to be taken into consideration. In this study, some closure correlations of the bubble departure diameter, active site density and bubble waiting time were tested in the frame of the two-fluid model and the CFX code. Benchmark experiments were then performed to evaluate the correlations. Comparison of the numerical results against the experimental data demonstrates that the surface tension is crucial to modeling the bubble departure diameter and the active site density. The bubble waiting time correlation formulated according to bubble growth is expected to be used as a criterion of judging the transition from subcooled to saturated boiling.

1. Introduction

The most important task when modeling subcooled boiling flow using a two-fluid model is to complement closure correlations describing interactions between the phases. During the past decades, although numerous literature deals with boiling flow of water using the two-fluid model, investigations of analogous phenomena in liquid nitrogen (LN_2) are very few since the closure correlations of nitrogen two-phase flow with phase change and the related numerical procedure have not been completely established.

In a subcooled boiling flow, bubble generation on the heating surface is the source of void in the two-phase flow field. It is crucial to supply closure correlations describing heat and mass transfer on the heating surface when modeling this process using a two-fluid model. Among them, the most important closure correlations appear to be those related to bubble nucleation, growth and departure, including the correlations of bubble departure diameter, bubble departure frequency, active site density, as well as the bubble growth and waiting time. Recently, the authors [1] demonstrated that the widely used closure correlations of heat and mass transfer on the heating surface during subcooled boiling flow of water is invalid to boiling flow LN_2 due to the differences in physical properties of the liquids. In fact, lots of investigations have demonstrated that the physical properties of the liquid have significant effect on the characteristics of bubble generation. For example, Kirichenko [2,3] and Bald [4] proved that in a nucleate boiling system the influence of contact angle on bubble departure is significant. For high-boiling liquids with large contact angle, vapor bubbles tend to break from the smooth surface, while for cryogenic liquids with small contact angle ($\phi \approx 0°$), bubbles tend to break from the cavity mouth and the cavity size has a significant effect on the bubble departure diameter. In fact, it is difficult to find a metal surface which would produce a value of $\phi > 7.5°$ in LN_2, therefore it can be expected the edge-break mechanism plays a predominant role in nucleate boiling of LN_2. Other experimental and theoretical investigations [3,5] demonstrated that the surface tension also has an important effect on bubble nucleation and departure.

Briefly, in order that an accurate two-fluid mechanism model of subcooled boiling flow of LN_2 can be formulated, the effect of physical properties of the liquid on bubble generation has to be taken into account. In this study, some new closure correlations related to heat and mass transfer on the heating surface are tested in the frame of the two-fluid model and the CFX-4.3 code. Benchmark experiments are then conducted in our laboratory to evaluate the correlations. The numerical results predicted with the correlations which take the effect of physical properties into account achieve satisfactory agreement with the experimental data.

* Corresponding author. Tel./fax: +86 21 3420 6055.
E-mail address: leexiangdong@sjtu.edu.cn (X. Li).

0017-9310/$ - see front matter © 2008 Elsevier Ltd. All rights reserved.
doi:10.1016/j.ijheatmasstransfer.2008.08.012

Nomenclature

A_c	area fraction subjected to convection (dimensionless)
A_q	area fraction subjected to quenching (dimensionless)
c_{pl}	specific heat of the liquid phase at constant pressure (J kg^{-1} K^{-1})
D	inner diameter of the tube (m)
d_c	cavity mouth diameter (m)
d_{bW}	bubble departure diameter (m)
d_g	diameter of a growing bubble (m)
f	bubble departure frequency $f = 1/(t_w + t_g)$ (s^{-1})
g	acceleration due to gravity (m s^{-2})
h_{fg}	the latent heat of evaporation (J kg^{-1})
Ja	the Jacob number, $Ja = \rho_l c_{pl}\Delta T/(\rho_v h_{fg})$ (dimensionless)
L	length of the tube (m)
n	the active site density (m^{-2})
p	absolute pressure (Pa)
p_{cr}	critical pressure of the liquid (Pa)
q	heat flux at the wall (W m^{-2})
q_c	heat flux due to convection (W m^{-2})
q_e	heat flux due to evaporation (W m^{-2})
q_q	heat flux due to quenching (W m^{-2})
T	temperature (K)
$T_{l,W}$	liquid temperature immediately next to the heating surface (K)
T_W	temperature of the heating surface (K)
ΔT_{sub}	liquid subcooling immediately next to the heating surface, $\Delta T_{sub} = T_{sat} - T_{l,W}$ (K)
ΔT_{sup}	wall superheating, $\Delta T_{sup} = T_W - T_{sat}$ (K)
t_g	bubble growth time (s)
t_w	bubble waiting time (s)
u_l	tangent liquid velocity in the cell immediately next to the heating surface (m s^{-1})

Greek letters

λ	heat conductivity (W m^{-1} K^{-1})
μ	molecular viscosity (Pa s)
ρ	density (kg m^{-3})
σ	surface tension coefficient (N m^{-1})

Subscripts

l	the liquid phase
sat	Saturated
sub	Subcooled
sup	Superheated
v	the vapor phase

2. Modeling of heat transfer at heating surface during subcooled boiling flow of LN_2

2.1. Heat flux partition on heating surface

Numerous investigations [6,7] demonstrated that the total heat flux q from per unit area of heating surface is partitioned into three components: heat flux due to evaporation q_e; heat flux due to quenching q_q and that due to convection q_c

$$q = q_c + q_e + q_q \tag{1}$$

where

$$q_e = \frac{\pi}{6} d_{bW}^3 \rho_v n f h_{fg} \tag{2}$$

$$q_q = A_q \frac{2}{\sqrt{\pi}} f \sqrt{t_w \lambda_l \rho_l c_{pl}} (T_W - T_{l,W}) \tag{3}$$

$$q_c = A_c St \rho_l c_{pl} u_l (T_W - T_{l,W}) \tag{4}$$

where f represents the bubble departure frequency and is modeled according to Kocamustafaogullari and Ishii [8]; A_q and A_c are, respectively, the area factions of the "bubble-influence region" and that of the convection controlled region, and are modeled according to Kenning [9]. The other parameters describing bubble nucleation and departure include the bubble departure diameter d_{bW}, the active site density n and the bubble waiting time t_w, which will be discussed in the following sections.

2.2. The bubble departure diameter

The bubble departure diameter d_{bW} is an important parameter in modeling nucleate boiling. Since LN_2 has a small contact angle ($\phi < 7.5°$) with most metallic surfaces, it is reasonable to assume according to Kirichenko [2,3] and Bald [4] that the edge-break mechanism predominates in nitrogen bubble departure and the bubble departure diameter is influenced by the size of the cavity mouth

$$d_{bW} = 2\left(\frac{3}{4}\frac{\sigma}{(\rho_l - \rho_v)g} d_c\right)^{1/3} \tag{5}$$

where d_c is the diameter of the active cavity mouth, which is decided by the local wall superheating [3]

$$d_c = \frac{4\sigma T_{sat}}{h_{fg}\rho_v \Delta T_{sup}} \tag{6}$$

For the purpose of comparison, the correlation of Tolubinsky and Kostanchuk (cited in [10]) is also incorporated in this study

$$d_{bW} = 0.014 \exp\left(\frac{\Delta T_{sub}}{45}\right) \tag{7}$$

2.3. The active site density

As mentioned above, physical properties of the liquid have a significant effect on nucleation. In this study, the formula proposed by Kirichenko [3] for the active site density in nucleate boiling of cryogenic liquids, which considers influence of the surface tension, is incorporated

$$n = C_n \left(\frac{h_{fg}\rho_v \Delta T_{sup}}{\sigma T_{sat}}\right)^m \tag{8}$$

where C_n and m depend on the pressure: $C_n = 1.0 \times 10^{-7}$, $m = 2$ when $p/p_{cr} \geqslant 0.04$ and $C_n = 625 \times 10^{-6}$, $m = 3$ when $p/p_{cr} < 0.04$, where p_{cr} is the critical pressure of the fluid.

For the purpose of comparison, the empirical correlation proposed by Lemmert and Chawla (cited in [11]), which is correlated only to the wall superheating, and the Kocamustafaogullari–Ishii [12] formula, which is a semi-empirical correlation for nucleate boiling of high-boiling liquids, but takes into account the influence of surface tension, are also included

$$n = [210\Delta T_{sup}]^{1.805} \tag{9}$$

and

$$n = \frac{f(\rho^*) R_c^{*-4.4}}{d_{bW}^2} \tag{10}$$

where

$$\rho^* = \frac{\rho_l - \rho_v}{\rho_v} \tag{11}$$

$$f(\rho^*) = 2.157 \times 10^{-7} \rho^{*-3.2}(1 + 0.0049\rho^*)^{4.13} \tag{12}$$

$$R_c^* = \frac{4\sigma T_{sat}}{\Delta T_{sup} \rho_v h_{fg} d_{bW}} \tag{13}$$

2.4. The bubble waiting time

The bubble waiting time t_w is defined as the time from a bubble departure to a sequential bubble nucleation at a same cavity. Due to the difficulty in modeling t_w, some investigators simply calculated it as

$$t_w = C_w / f \tag{14}$$

where C_w is an empirical constant. Agreement has not been achieved in selecting the value of C_w, for example, different values such as $C_w = 0.8$ [11] and $C_w = 1.0$ [10] have appeared in the literature.

After a bubble departs, the newly filled liquid has to be heated up to a temperature slightly higher than the local saturation temperature for a sequential bubble nucleation. As a result, t_w is factually the time that the quenching mechanism persists during a bubble period. It can be expected that t_w decreases with reduced liquid subcooling. As the bulk liquid approaches its saturation temperature, evaporation occurs as soon as the liquid gets contact with the superheated surface, the bubble waiting time approaches zero and the quenching mechanism eliminates. Here, a simple method calculating t_w is put forward according to the growth rate of cryogenic bubbles.

Numerous investigations [3,5,13–15] have proved that for nucleate boiling of cryogenic liquids, the size of a growing bubble is in proportion to the square root of the growing time ($d_g \sim \sqrt{t}$). The validity of Scriven's correlation for nitrogen bubble growth rate has been verified by Bald [15], therefore, it is employed here

$$d_g = 4\sqrt{\frac{3}{\pi}} \frac{\rho_l c_{pl} \Delta T_{sup}}{\rho_v [h_{fg} + (c_{pl} - c_{pv}) \Delta T_{sup}]} \sqrt{a_l t} \tag{15}$$

where a_l is thermal diffusivity of the liquid ($a_l = \lambda_l / (\rho_l c_{pl})$). Substituting d_g in Eq. (15) by the bubble departure diameter d_{bW}, the bubble growth time t_g can be decided and hence the bubble waiting time t_w

$$t_w = 1/f - t_g \tag{16}$$

3. The experiments

In order to evaluating the closure correlations, an experimental rig is built up in our laboratory and benchmark experiments are conducted. The structure of the experimental rig and the experimental procedure have been detailedly highlighted elsewhere [16], only a brief description of the test section is given here.

The test section is illustrated in Fig. 1, which is a circular tube made of 304# stainless steel (0Cr18Ni9), with an inner diameter of 6.0 mm, a wall thickness of 1.0 mm and an effective length of 1000 mm. The tube is connected to an upstream stabilizer and to a downstream top cover using flanges. The test section is electrically heated using a heating belt wrapped on the outer surface and the heating power is controlled using an adjustable power system. Seventeen groups of copper-constantan thermocouples are equally fixed on the outer surface of the test section along the length at every distance of 60 mm. Each group includes four thermocouples which are equally fixed in a circumference. The thermocouples were carefully calibrated before installation using a standard platinum resistance thermometer. The calibrating

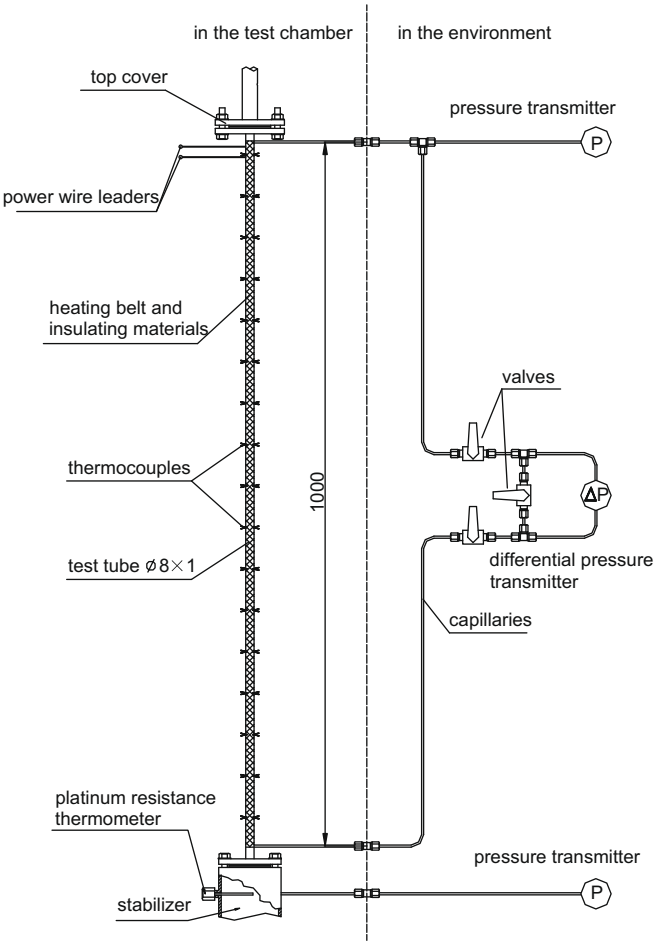

Fig. 1. Schematic diagram of the test section.

results showed that the accuracy is better than 0.1 K. When axial heat conduction is neglected, the temperature of the inner surface of the tube can be decided according to the records of the thermocouples, together with the heat flux and the wall thickness.

A platinum resistance thermometer with an accuracy of 0.1 K and a pressure transmitter with a measuring range of 0–3.0 MPa and an accuracy of 0.5% are installed in the stabilizer. Another pressure transmitter with the same range and accuracy as that installed at the stabilizer was installed near the outlet of the test section.

In the benchmark experiments, operating parameters including the outlet pressure, the heat flux and the mass flow rate are carefully selected. The outlet pressure varies from 0.195 to 1.129 MPa and the mass flux is in the range of 184.7–584.8 kg/(m^2 s). The inlet liquid subcooling during the experiments appears in the range of 0.87–10.61 K. The heat flux is in the range of 1026–30,125 W m^{-2}.

Due to the inherent instability of two-phase flows, the readings of the instruments keep fluctuating, but the average values of the readings are almost constants. Therefore, the records are acquired at a sampling frequency of 1.0 Hz for at least 30 min and the time-averaged values of the records are used as the computational conditions and the benchmark data. Details of the experimental data are shown in Table 1.

4. Results and discussion

4.1. Numerical computations

The commercial CFD code CFX-4.3 is used as a frame to perform the computations and to evaluate the models. The above closure

Table 1
Details of the experimental data

Experimental case No.	Outlet pressure (abs) (MPa)	Mass flow rate (kg m^{-2} s^{-1})	Heat flux (W m^{-2})	Inlet subcooling (K)
1	1.129	584.6	25,216	10.6
2	1.129	585.2	30,125	10.6
3	1.129	584.6	23,291	10.6
4	0.710	185.9	2049	2.2
5	0.343	371.8	3873	3.3
6	0.195	288.6	1026	0.9

equations are incorporated in the two-fluid model through the CFX user-defined subroutines and two-dimensional numerical simulations are performed. Details of the two-fluid model and the numerical procedure have been highlighted in the authors' earlier publication [1,16] and will not be repeated here. The boundary conditions of the computations are from the experimental data, which are listed in Table 1. Before evaluating the closure correlations, the sensitivity of grid density is firstly analyzed. Due to the axial symmetry of the two-phase flow field, a two-dimensional computational domain with a dimension of 3×1000 mm is built and three different grid arrangements (5×1000, 10×1000 and 15×1000 uniform rectangular cells) are tested. It is found that there is no significant difference between the predicted results of the 10×1000 and those of the 15×1000 grid arrangements. Therefore it is confirmed that the 10×1000 grid arrangement is adequate to the issue of this study.

4.2. Influence of the bubble departure diameter

When evaluating the influence of bubble departure diameter, the formula proposed by Tolubinsky and Kostanchuk (Eq. (7)) and that by Kirichenko (Eq. (5)) are, respectively, incorporated, while other models and parameters are kept unchanged. As shown in Fig. 2(a), both the models predict decreasing bubble departure diameter along the flow, but Eq. (7) predicts a larger bubble departure diameter than Eq. (5). Many experimental observations [3,15] demonstrated the bubble departure diameter of nitrogen bubble in nucleate pool boiling is less than 0.5 mm. Although no experimental data on d_{bW} is available in this study, it can be expected that d_{bW} in flow boiling is smaller than that in pool boiling due to the liquid inertia force [17] and therefore $d_{bW} < 0.5$ mm persists. The Tolubinsky–Kostanchuk model tends to over-predict d_{bW} during boiling of LN_2 mainly due to the fact that it fails to take into account the cavity-break mechanism.

However, in flow boiling systems, many factors including the liquid velocity, system pressure, heat flux and physical properties of the liquid and the surface material have strong effects on the bubble departure diameter. At present, few experimental data are available to formulate an accurate model for d_{bW} during boiling flow of LN_2 and further study is urgently needed.

It seems according to Fig. 2(b) that the bubble departure diameter models have no significant effect on the evolution of wall temperature after nucleate boiling is initialized. Further study showed that the wall temperature is mainly decided by the active site density modeling, which will be discussed in the following sections.

4.3. Influence of the active site density

Prior to evaluating the active site density models, it is helpful to understand the influence of surface profile of the heating solid and physical properties of the liquid on bubble nucleation.

A typical probability density function (PDF) of cavity mouth diameter on a commercially manufactured stainless steel surface follows the Weibull distribution, as shown in Fig. 3, which was obtained by Qi et al. [18] using a vertical scanning interferometer. Although cavities with a wide range of sizes exist on the surface, only those in a certain size range ($d_{c,min} \leqslant d_c \leqslant d_{c,max}$) can be activated. The minimum active cavity mouth diameter $d_{c,min}$ is related to the local wall superheating and the liquid surface tension by $d_{c,min} \sim \sigma/\Delta T_{sup}$ [19]. The maximum active cavity mouth diameter $d_{c,max}$ is decided by the contact angle, since only cavities capable of capturing gases can develop to nuclei while those with size beyond $d_{c,max}$ would be flooded by the liquid [6,20]. Tong [21] and Cornwell [22] demonstrated that the effect of contact angle is significant for highly wetting liquids. Accordingly, it can be expected that with reduced surface tension and contact angle, both $d_{c,min}$ and $d_{c,max}$ decrease and the zone of active sites moves left in Fig. 3, which illustrates that the probability density of small cavities is much larger than that of large cavities, therefore means larger active site density.

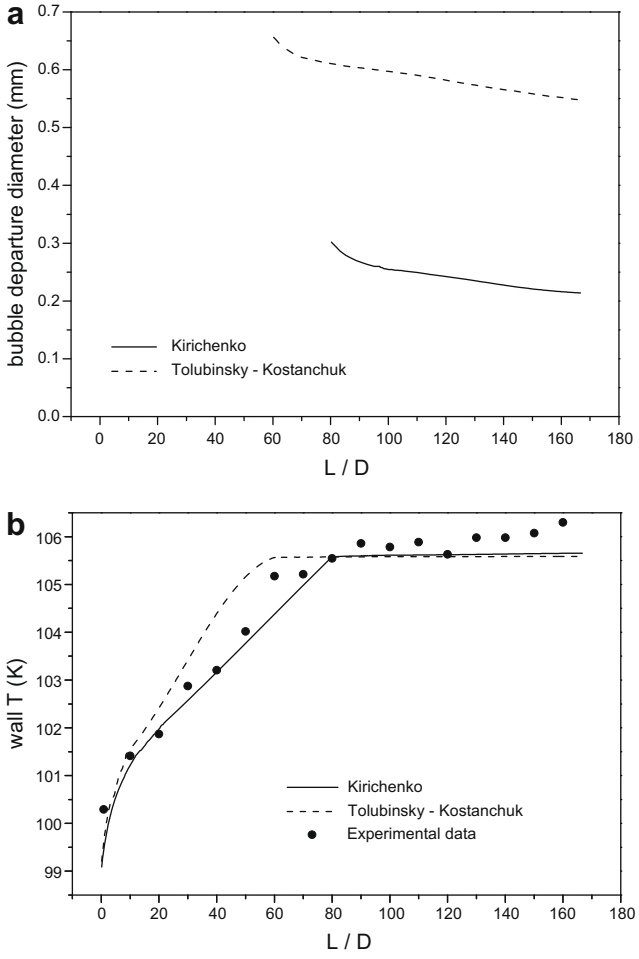

Fig. 2. Influence of bubble departure diameter (Case 1) (a) bubble departure diameter and (b) wall temperature.

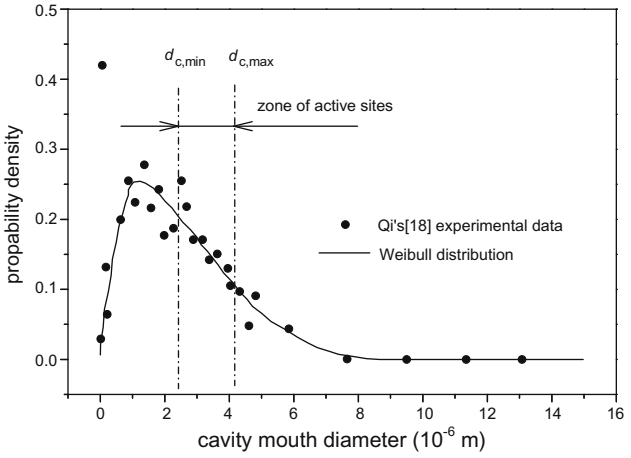

Fig. 3. Typical PDF of cavity mouth diameter distribution on a stainless steel surface [18].

Fig. 4 shows comparison of the numerical results predicted using Eqs. (8)–(10), respectively, while other models and parameters are kept unchanged. It is found that the effect of the surface tension is significant in modeling nucleate boiling of LN_2. Due to failing to take into account the influence of physical properties, the Lemmert–Chawla equation (Eq. (9)) under-predicts the active site density (Fig. 4(a)), which leads to an error in prediction of the liquid temperature. As shown in Fig. 4(b), where the liquid temperature is defined as the temperature of liquid averaged over a cross-section, the liquid temperature predicted by Eq. (9) largely exceeds the saturation temperature and keeps rising, which is obviously physically untrue. The Kirichenko model (Eq. (8)) and the Kocamustafaogullari–Ishii model (Eq. (10)) predict higher active site density and more rational parameter evolutions.

Although the both models predict similar evolution tendencies in liquid temperature and wall temperature (in Fig. 4(b) and (c)), the Kirichenko model predicts a larger active site density than the Kocamustafaogullari–Ishii model (Fig. 4(a)). As a result, there arises a problem that which model is more accurate in describing the active site density in nucleate boiling of LN_2. Since no quantitative experimental data are available, further computations are performed to evaluate the models in the range of pressure 0.195–1.129 MPa, inlet subcooling 0.87–10.61 K and mass flux 185.9–584.6 kg/(m^2 s), as shown in Fig. 5.

According to Fig. 5, it seems that the Kirichenko model generates better predictions, especially at lower pressure. Although both the Kirichenko model and the Kocamustafaogullari–Ishii model take into account the effect of contact angle, the former was formulated according to experimental data of cryogenic liquids while the latter was established on the base of high-boiling liquids. The main cause that leads the Kocamustafaogullari–Ishii model to error when predicting the active site density during nucleate boiling of LN_2 may lies in Eq. (12).

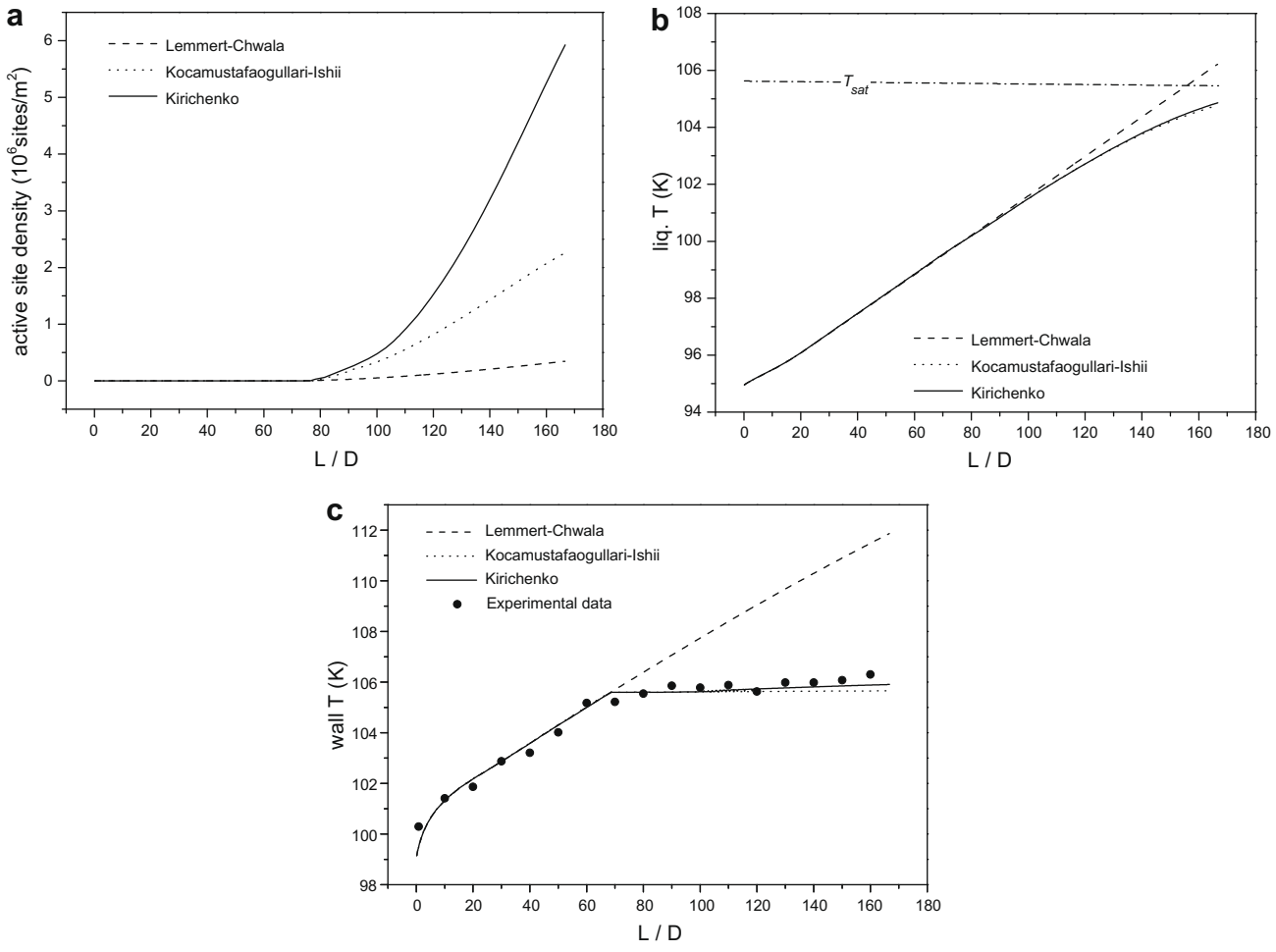

Fig. 4. Influence of the active site density (Case 1) (a) the active site density, (b) liquid temperature and (c) wall temperature.

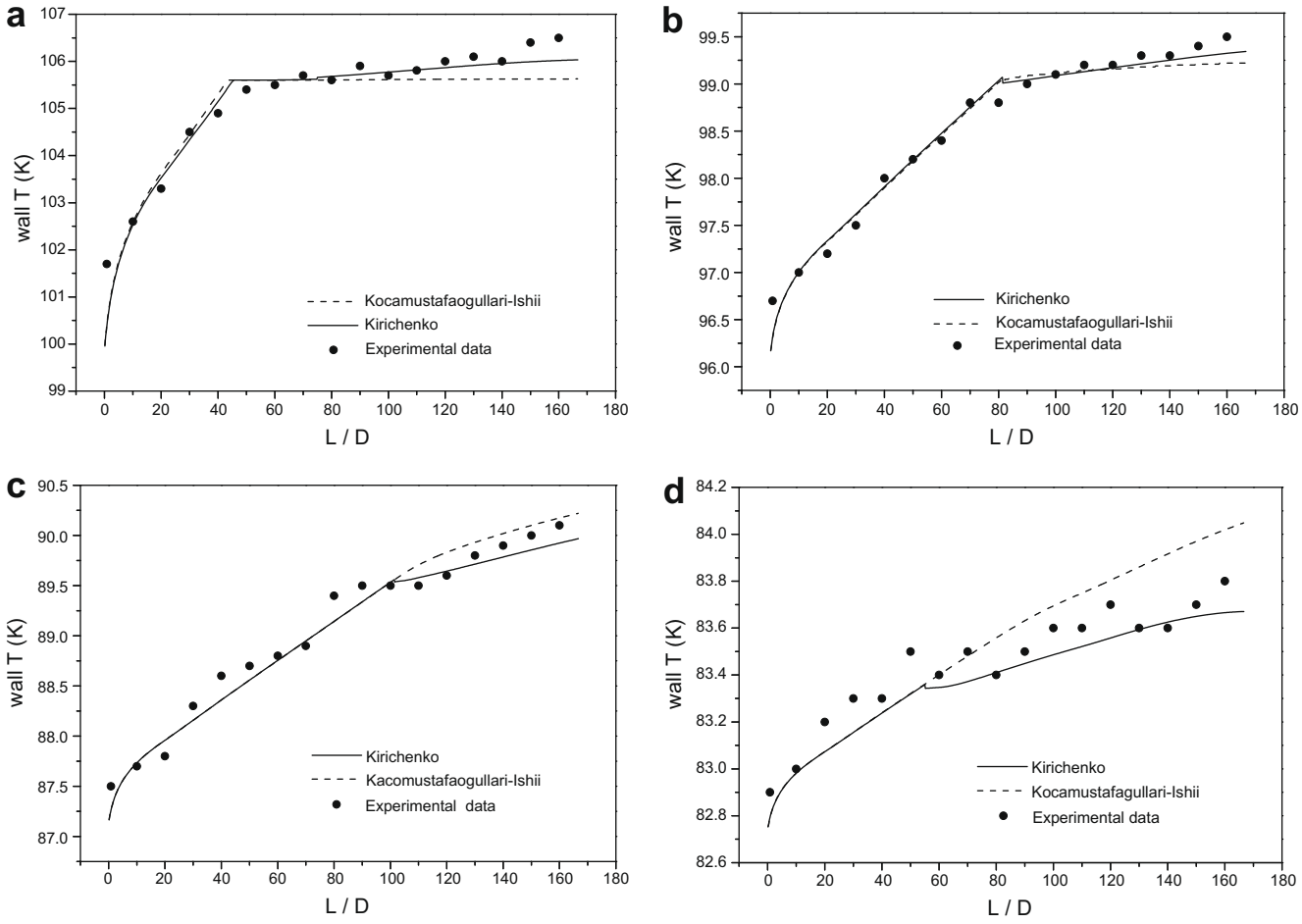

Fig. 5. Comparison of predicted wall temperature against experimental data (a) Case 2, (b) Case 4, (c) Case 5 and (d) Case 6.

4.4. Influence of the bubble waiting time

The influence of bubble waiting time models is analyzed by employing Eq. (14) with $C = 0.8$ (denoted as "empirical" in Fig. 6), and the equation used by the authors (Eq. (16), denoted as "mechanistic" in Fig. 6), respectively, while other models and parameters are kept unchanged. Fig. 6 shows comparison of the numerical results, where the dimensionless bubble waiting time is defined by

$$t_w^* = \frac{t_w}{1/f} \tag{17}$$

It can be seen according to Fig. 6(a) that the empirical equation predicts a constant dimensionless bubble waiting time ($t_w^* = 0.8$) while the mechanistic model predicts a decreasing t_w^*. Especially as shown in Fig. 6(b), the equations predicted inverse evolving tendencies of quenching heat transfer coefficient. Although there is no quantitative benchmark data on the quenching heat transfer coefficients available, it can be judged that the Eq. (16) is more physically rational according to the descriptions in Section 2.4.

Although the numerical predictions show that the bubble waiting time plays a minor role in predicting the wall temperature (as shown in Fig. 6(d)), the quenching mechanism is publicly acknowledged very important in subcooled boiling flow. The authors expect that the dimensionless bubble waiting time t_w^* may be used as a useful criterion for judging the transition from subcooled to saturated boiling since the quenching mechanism appears mainly in subcooled boiling.

5. Conclusion

When simulating subcooled boiling flow using a two-fluid model, one has to supply the closure correlations describing heat transfer from the heating surface to the fluids. Although lots of empirical or semi-empirical correlations have been established for subcooled boiling flow of high-boiling liquids, these correlations may be invalid when modeling subcooled boiling flow of LN_2, mainly due to the difference in physical properties of the liquids. In this job, some closure correlations for the bubble departure diameter, active site density and bubble waiting time are tested and numerical simulations are performed in the frame the CFX code. Benchmark experiments show that the correlations considering this difference achieve satisfactory agreement with the experimental data. The main conclusions rising from this study are as follows:

(1) LN_2 has a small surface tension and contact angle, which is the main reason leading to smaller bubble departure diameter and higher active site density. When modeling nucleate boiling of LN_2, it is crucial to take into account the effects of surface tension and contact angle.
(2) Among the nucleate boiling parameters investigated in this study, modeling of the active site density has the most significant effect on predicting temperature of the heating surface.
(3) The bubble waiting time decreases with reduced liquid subcooling. When saturated boiling occurs, it approaches zero. Therefore, t_w is expected to be used as a criterion for judging the transition from subcooled to saturated boiling.

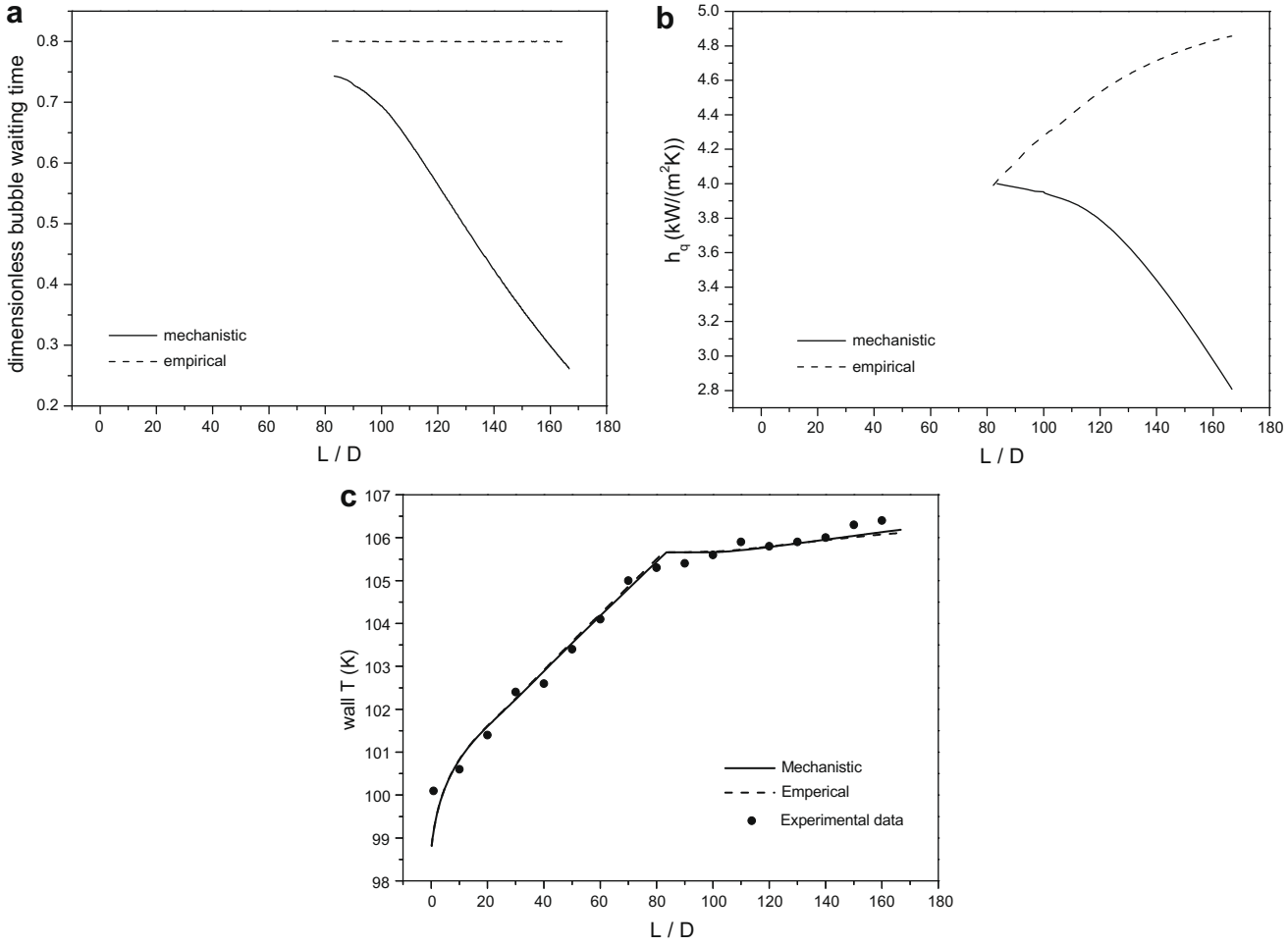

Fig. 6. Influence of the bubble waiting time (Case 3) (a) dimensionless bubble waiting time, (b) quenching heat transfer coefficient and (c) wall temperature.

Acknowledgement

The financial supports from the Postdoctoral Scientific Funds of China (20070410722) are gratefully acknowledged.

References

[1] X.D. Li, R.S. Wang, R.G. Huang, Y.M. Shi, Numerical investigation of boiling flow of nitrogen in a vertical tube using the two-fluid model, Appl. Thermal Eng. 26 (17–18) (2006) 2425–2432.
[2] Yu. A. Kirichenko, L.A. Slobozhanin, N.S. Shcherbakova, Analysis of quasi-static conditions of boiling onset and bubble departure, Cryogenics 23 (2) (1983) 110–112.
[3] Yu. A. Kirichenko, M.L. Dolgoy, N.M. Levchenko, et al., Study of the boiling of cryogenic liquids, Heat Transfer Soviet Res. 8 (4) (1976) 63–72.
[4] W.B. Bald, Cryogenic heat transfer research at Oxford, part 1 – nucleate pool boiling, Cryogenics 13 (8) (1973) 457–469.
[5] V.A. Grigoryev, Yu. M. Pavlov, E.V. Ametistov, et al., Investigation of the growth rate of vapor bubbles in the boiling of cryogenic fluids, Heat Transfer Soviet Res. 7 (5) (1975) 133–140.
[6] N. Basu, G.R. Warrier, V.K. Ghir, Wall heat flux partitioning during subcooled flow boiling: part 1 – model development, J. Heat Transfer 127 (2) (2005) 131–140.
[7] AEA Technology plc, CFX-4.3 Solver Manual, Harwell, United Kingdom, 1999.
[8] G. Kocamustafaogullari, M. Ishii, Foundation of the interfacial area transport equation and its closure relations, Int. J. Heat Mass Transfer 38 (3) (1995) 481–493.
[9] D.B.R. Kenning, H.D.V.M. Victor, Fully developed nucleate boiling: overlap of areas of influence and interference between bubble sites, Int. J. Heat Mass Transfer 24 (6) (1981) 1025–1032.
[10] J.Y. Tu, G.H. Yeoh, On numerical modelling of low-pressure subcooled boiling flows, Int. J. Heat Mass Transfer 45 (6) (2002) 1197–1209.
[11] B. Koncar, I. Kljenak, B. Mavko, Modelling of local two-phase flow parameters in upward subcooled flow boiling at low pressure, Int. J. Heat Mass Transfer 47 (6–7) (2004) 1499–1513.
[12] G. Kocamustafaogullari, M. Ishii, Interfacial area and nucleation site density in boiling system, Int. J. Heat Mass Transfer 26 (9) (1983) 1377–1387.
[13] L. Bewilogua, R. Knöner, H. Vinzelberg, Studies on bubble formation in low boiling liquids, Cryogenics 10 (1) (1970) 69–70.
[14] W.B. Bald, Bubble growth constant for liquid hydrogen and liquid helium, Cryogenics 16 (12) (1976) 709–712.
[15] M.E. Bland, C.A. Bailey, G. Davey, Boiling from metal surfaces immersed in liquid nitrogen and liquid hydrogen, Cryogenics 13 (11) (1973) 651–657.
[16] X.D. Li, R.S. Wang, R.G. Huang, Y.M. Shi, Numerical and experimental investigation of pressure drop characteristics during upward boiling two-phase flow of nitrogen, Int. J. Heat Mass Transfer 50 (9–10) (2007) 1971–1981.
[17] L.Z. Zeng, J.F. Klausner, D.M. Bernhard, et al., Unified model for the prediction of bubble detachment diameters in boiling systems – II flow boiling, Int. J. Heat Mass Transfer 36 (9) (1993) 2271–2279.
[18] Y. Qi, J.F. Klausner, R. Mei, Role of surface structure in heterogeneous nucleation, Int. J. Heat Mass Transfer 47 (14–16) (2004) 3097–3107.
[19] G.E. Thorncroft, J.F. Klausner, R. Mei, Suppression of flow boiling nucleation, J. Heat Transfer 119 (3) (1997) 517–526.
[20] N. Basu, G.R. Warrier, V.K. Ghir, Onset of nucleate boiling and active nucleation site density during subcooled flow boiling, J. Heat Transfer 124 (4) (2002) 717–728.
[21] W. Tong, A. Bar-Cohen, T.W. Simon, et al., Contact angle effect on boiling incipience of highly-wetting liquids, Int. J. Heat Mass Transfer 33 (1) (1990) 91–103.
[22] K. Cornwell, R.B. Schuller, A study of boiling outside a tube bundle using high speed photography, Int. J. Heat Mass Transfer 25 (5) (1982) 683–690.